Preparation and patterning of nanoscale hybrid materials for micro-optics

P. OBREJA[a*], D. CRISTEA[a], V. S. TEODORESCU[b], A. DINESCU[a], A.C. OBREJA[a], F. COMANESCU[a], R.REBIGAN[a]

[a] National Institute for R&D in Microtechnologies (IMT-Bucharest), 126A Erou Iancu Nicolae 077190, Bucharest-Voluntari, Romania,
[b] National Institute of Materials Physics, PO Box MG. 7, 77125, Magurele, Bucharest, Romania

The refractive index of organic polymers can be modified by incorporation of inorganic nanoparticles with higher or lower refractive index. The paper presents our experimental results regarding the preparation of hybrid nanocomposite films with controlled refractive index for micro-optics and integrated optics. These materials were obtained by chemical routes and sol-gel processes from commercial polymers (PMMA, PVA), metal (Ag), metal oxide nanoparticles (TiO$_2$, ZrO$_2$) or organic materials (Rhodamine, Alq3). The properties of these materials depend on the composition, metal/oxide concentration, particle size and dispersion homogeneity. The hybrid nanocomposite films were characterized using spectroellipsometry, UV-VIS spectroscopy, AFM, TEM and the optical properties were correlated with processing parameters. Micro/nano pattering techniques based on combination of electron beam lithography and replication techniques have been developed to obtain structures with applications in micro-optics. Components like micro-lenses, diffractive optical elements and optical waveguides have been obtained and characterized using SEM and AFM.

1. Introduction

Polymers play an important role in photonic applications due to their excellent properties like low dielectric constant dispersion, high bandwidth, high packaging density, low cost, compatibility with various patterning methods and ease of fabrication. Polymers can be used as materials due to their individual refractive index and transmittance or as matrices for optically active species that customize their optical properties. Polymers in combination with inorganic nanoparticles (e.g. oxides, metals, semiconductors) or other organic materials (e.g. dyes, liquid crystals) are of particular interest in photonic for solar cells [1-3], light emitting diodes [4], optical sensors [5,6], optical data storage [7-9], optical data communication (e.g. planar optical waveguide in local networks) and for other applications [10-12].

A nanocomposite polymer has novel mechanical, electronic, chemical or optical properties. Their optical properties can be tailored by dispersing the inorganic nanoparticles or by solving an organic dopant in the polymer matrix and depend on its composition, structure, size and shape of the nanoparticles included in polymer [13-16].

The patterning of nanocomposite polymers films at micro and nanometre scales can be done by electron beam lithography and soft lithographic techniques [17-20].

Taking into account the diversity of compositions used for nanocomposite polymers, in the present paper a study regarding the correlation between the composition and the optical properties and patterning techniques for PVA-Ag, and PMMA doped with metal oxides (TiO$_2$, ZrO$_2$) or organic dyes (Alq3, Rhodamine) was carried out and the experimental data is reported.

2. Experimental

2.1. Materials and preparation techniques

All chemical reagents including poly(methyl methacrylate) (PMMA with molecular weight M_w = 120000 and M_w = 950000), polyvinyl alcohols (PVA with M_w = 31 000-50000), 2-hydroxyethyl methacrylate (HEMA), methyl methacrylate (MMA), titanium (IV) isopropoxide (97 wt. % purity), zirconium(IV) propoxide (70 wt. % solution in 1-propanol), acetylacetone (99 wt. % purity) and other chemicals were used as received (from Aldrich) without further purification.

Silver-polymer nanocomposites were prepared by chemical route. PVA was dissolved in deionised water under stirring and heating at 70 ^{o}C and then filtered through serigraphic silk. 10% silver nitrate (AgNO$_3$) aqueous solution was added in 5% PVA aqueous solution in three different volumetric ratios: 1:10, 2:10 and 3:10. The PVA-AgNO$_3$ solutions were spin coated on glass and on oxidized silicon wafer substrates at 3000 rpm for 60 seconds and the films were UV exposed at 405 nm wavelength with 7mW/cm^2 dose for 10 min., for reduction of silver ions to silver metal.

Metal oxide-polymer nanocomposites were prepared by sol-gel process, starting from polymers

solutions and alkoxides, at room temperature and under nitrogen atmosphere. PMMA-TiO$_2$ nanocomposites were obtained from PMMA solutions (in chlorobenzene or in methylmethacrylate) and titanium isopropoxide chelated with acetylacetone (in different molar ratio) in order to increase the concentration of TiO2 and to improve the nanoparticle dispersion in the polymer films, to control the hydrolysis/condensation reactions and implicit to control the TiO$_2$ nanoparticle - polymer interface.

PMMA-ZrO$_2$ nanocomposites were prepared using the same PMMA solution and zirconium propoxide in isopropanol, chelated with acetylacetone in molar ratio 1:10:2.

PMMA-organic dopants were obtained by adding in 7% PMMA solution in chlorobenzene rhodamine B 0.5% solution in ethyl alcohol or 0.5% Alq3 in chlorobenzene: ethyl alcohol (volumetric ratio 1:1).

2.2. Nanocomposite films characterization

The relevant optical characteristics of the nanocomposite films were measured using UV-VIS spectroscopy for the transmittance and ellipsometry measurements to determine the refractive index and the thickness of the thin film.

The size and the dispersion of the nanoparticles in the polymer matrix were estimated using transmission electron microscopy (TEM) and atomic force microscopy (AFM). The TEM specimens were prepared by cross section technique using mechanical poliching and ion thinning in a Gatan PIPS aparatus.

Optical, confocal microscopy, atomic force microscopy (AFM) and scanning electron microscopy (SEM) were used to estimate the topography of patterned nanocomposite films with micro and sub-micron feature size details.

2.3. Polymer films patterning

The patterning of nanocomposite polymers films at micro and nanometre scales can be made by electron beam lithography (EBL), nanoimprint lithography (NIL) [11], inkjet printing and soft lithographic techniques developed as alternatives for photolithography [17-21].

Very low doped PMMA layers were easily patterned by EBL. For high dopant concentration, EBL is not possible (the presence of the dopant doesn't allow a good development). That is why we have experimented microtransfer molding technique to pattern PMMA nanocomposites. In microtransfer molding, a PDMS stamp is filled with a polymer solution and placed on a substrate. The material is cured and the stamp is removed. The technique generates features as small as 250 nm.

PDMS molds (or stamps) were fabricated by mixing the base and the curing agent Sylgard 184 (Dow-Corning) in weight ratio 10:1, further degassing and poured on the photoresist based master obtained by

optical lithography. The stamps were peeled away from the master after curing at 60°C for 3 hrs. A drop of the doped PMMA solution fills the channels of PDMS mold and then the stamp is placed on the substrate. The stamp is removed after material curing and the aspect of the replica in doped PMMA is characterized by optical methods. This technique can be used for any polymer based not only for PMMA. The original (master) can be obtained in resist or silicon. For the first experiments, we used a SU-8 master obtained by UV lithgraphy.

As PMMA-TiO$_2$ nanocomposites are more sensitive than PMMA, a photolithography of PMMA-TiO$_2$ nanocomposite film was experimented. In a solution prepared from PMMA in monomer and titanium isopropoxide chelated with acetylacetone was added a photoinitiator for UV curing (1-hdroxy-cyclohexyl-phenyl-ketone solution in MMA). The solution was spin coated onto the substrate, UV exposed through a mask at 7 mW/cm^2, 8 minutes and developed in methyl isobutyl ketone (MIBK).

3. Results and discussion

3.1. PMMA nanocomposites

PMMA-TiO$_2$, PMMA-ZrO$_2$ nanocomposites were prepared by sol-gel process. The optical properties of the nanocomposites were analysed by spectroellipsometry and spectroscopy in the UV-Vis-near IR range.

The modelling of the experimental ellipsometric spectra for the nanocoposites was done with the multicomponent Bruggeman's Effective Medium Approximation model. The fit parameters were the thickness of the layer and the volume fraction of the components; the values of these parameters for the experimental samples are presented in table 1. From the best fit, we obtained the refractive index presented in Fig. 1.
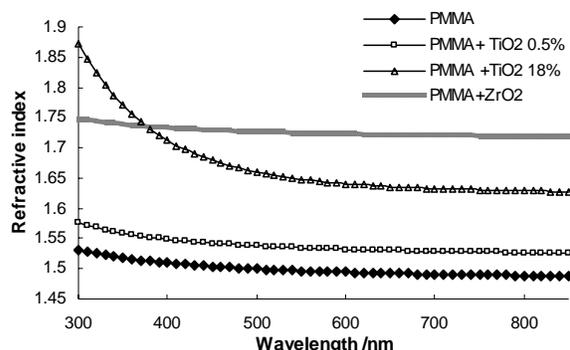
Fig.1. Dispersion of the refractive index of PMMA doped with TiO$_2$ (low concentration and high concentration), or ZrO$_2$

One can see that a significant increase of the PMMA refractive index was obtained, even for low dopant concentration. Thus, we are able to increase the

refractive index at λ = 630 nm from 1.49 to 1.53 by adding a very small quantity of TiO_2 (0.5%) and up to 1.63 by increasing the dopant concentration.

A more significant increase was obtained by doping with ZrO_2 up to 1.72 at λ = 630 nm. The highly doped PMMA with ZrO_2 has a high refractive index, with a very low dispersion in the range 300-900 nm because ZrO_2 shows a low variation of n with wavelength. These layers with high refractive index can be used these to fabricate photonic components like PMMA-based high contrast waveguides, and photonic crystals on oxidized silicon.

The layers have a very good uniformity (thickness variation less than 1.5%, see table 1).

The spectrophotometric measurements (transmittance and absorbance) indicated that the addition of the dopant does not have a significant influence on the transmittance in the range 400-900 nm (decrease less than 5% even at high dopant concentration) in comparison with pure PMMA.

Table 1 Thickness and dopant concentration for the experimental samples.

Sample	Thickness	Volume fraction of the dopant
PMMA doped with TiO_2- high concentration	3360±127 nm	18.5%
PMMA doped with TiO_2- low concentration	871 ± 12nm	0.5%
PMMA doped with ZrO_2	905 ±15	29%
PMMA doped with Alq3	464± 6nm	1%
PMMA doped with Rhodamine	517±4 nm	0.4%
PVA doped with 3.8%Ag	81±3nm	5.4%
PVA doped with 4.6%Ag	73±4nm	4.6%

The results of the spectroellipsometric measurements for the PMMA layers doped with dyes (Alq3 and Rhodamine) are given in Fig. 2 and Table 1. The model used was multicomponent Bruggeman Effective Medium Approximation. The films uniformity is also very good – thickness variation less than 1% (table 1).

For these films, doped with Rhodamine and Alq3 there is an anomalous dispersion around 550nm and 400 nm respectively, due to the specific absorbance of the dopants.

One can see that in the transparency region, Alq3 doped PMMA shows an increase of the refractive index in comparison with PMMA. For Rhodamine doped PMMA this increase is more obvious for λ > 600 nm.

These materials can be used not only for fluorescence based sensors, and emitting devices [4], but also for high contrast waveguides in combination with pure PMMA or SiO_2.
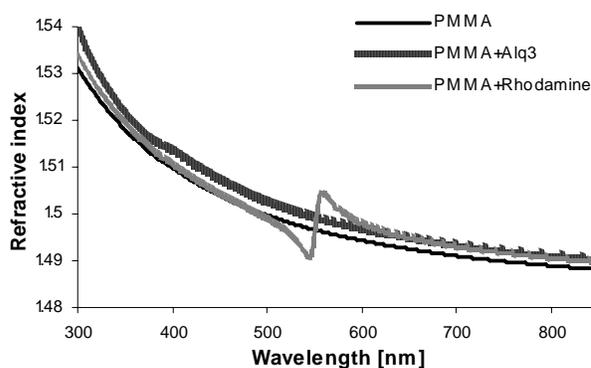
Fig.2 Dispersion of the refractive index of dye doped PMMA

The size and the dispersion of TiO_2 in the PMMA films were estimated by transmission microscopy (TEM). As one can see from fig.3, for small concentration, TiO_2 precipitates are uniform dispersed in the film. The size of TiO_2 precipitates is approximately 5 nm in diameter. EDX analysis on this zone shows titanium traces at the limit of detectable signal (fig.4).

At highest concentration TiO_2 (e.g. 18.5%), the nanocrystalite density is higher and some crystallites grow up to about 10 nm. The film morphology become nonuniforme and porous (fig.5).
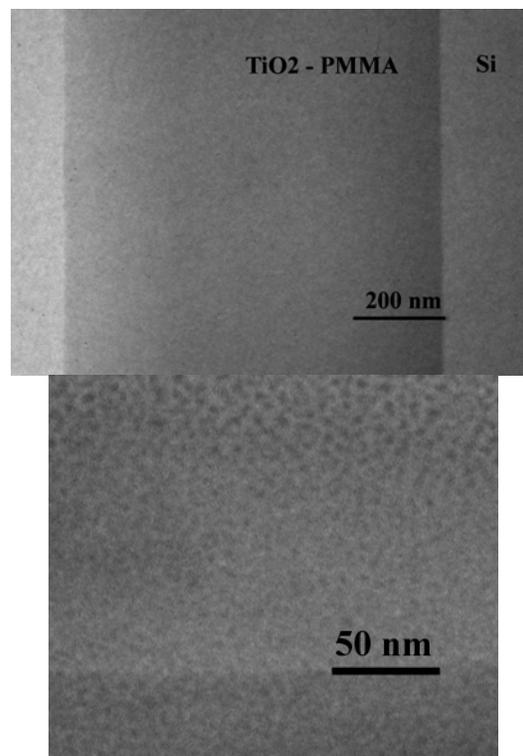
Fig.3. Low magnification XTEM image (left) and high magnification detail (right) of PMMA - 0.5%TiO_2 at the PMMA layer on SiO_2/Si[100] wafer.
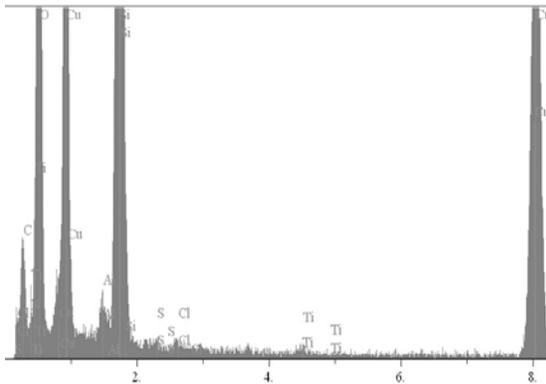
Fig.4. EDX spectrum for PMMA - 0.5%TiO₂ on the zone
presented in fig.3
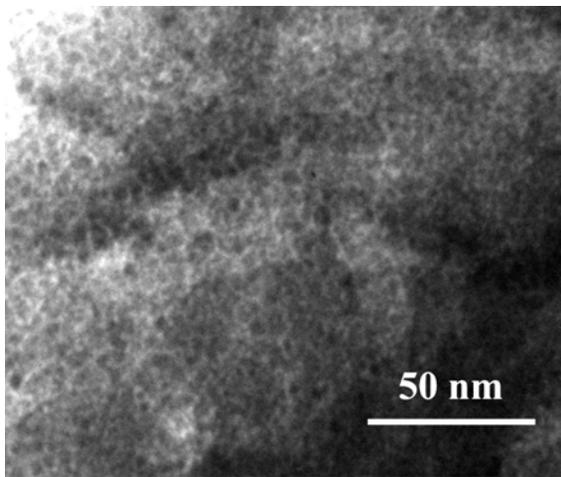
Fig. 5. XTEM image of PMMA – 18.5% TiO2 film,
detail of the top film area.

3.2. PVA based nanocomposites

PVA-Ag nanocomposites have been developed using a chemical route, by in-situ formation of metal nanoparticles within the polymer matrix, after the films were UV exposed. It has been observed that the nanoparticles tend to aggregate and form clusters during the preparative process.

The real and imaginary refractive index of the PVA doped with Ag (two concentrations) is given in fig. 6 and the transmittance in fig. 7. The shape of the curves indicates the presence of Ag nanoparticles. The absorption is resonantly enhanced at the dipole particle plasmon resonance [22].

One can see that for λ >600 nm the absorbance is rather low and the refractive index shows an important increase, so the layers are suitable for waveguide and photonic crystals fabrication.

The plasmonic behavior and the application in plasmonic devices of these layers will be the subject of further investigation.
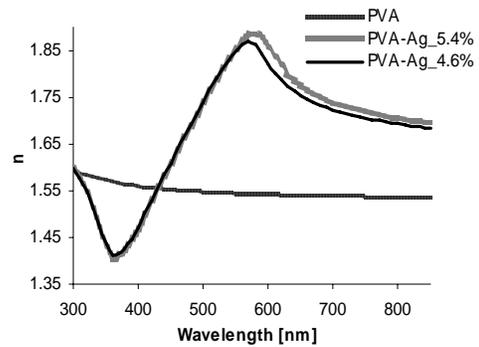
a)
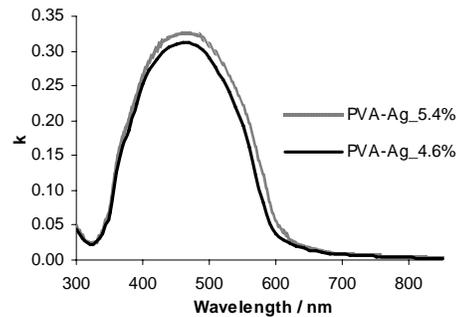
b)

Fig. 6. Dispersion of the real (a) and imaginary (b)
refractive index of the Ag doped PVA

Fig. 8 shows the TEMimages of PVA –Ag nanocomposites (two cAg concentrations).

As one can seen from pictures presented in fig.6-8, the refractive index and the transmittance of PVA-Ag films depend on Ag contend in the films, while the size of nanoparticles (6-20 nm) seems to be not depending from the Ag concentration. The density of nanoparticles is different between the two probes presented in fig.8, while the size of Ag nanoparticles is similar in the two probes. On can suppose that the number of nucleation centres depend on initial silver concentration and the size of Ag nanoparticles depends on the nanocristalites growth process. The XTEM image in figure 9 reveals also that the nucleation sites for the Ag crystallites are preferentially distributed on the both surfaces of the deposited film.
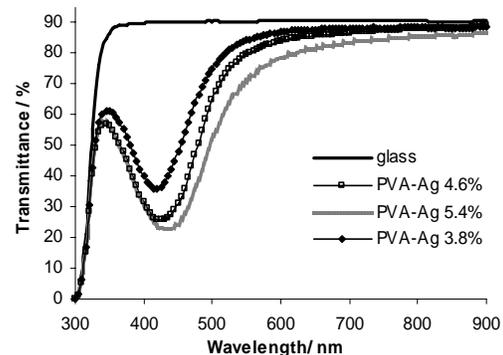
Fig.7. Transmittance (a) and absorbance (b) of the Ag
doped PVA
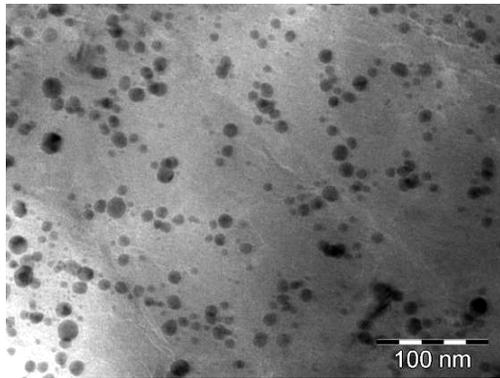
a)
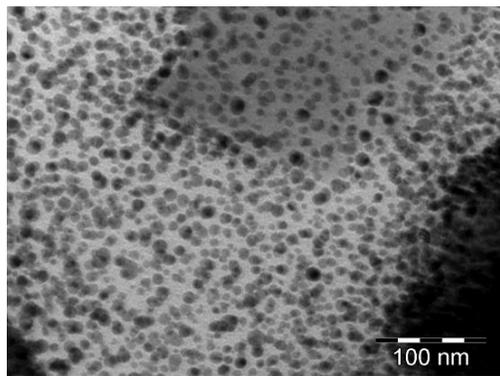
b)

Fig. 8. Plan view TEM images (comparative) on PVA-Ag;a) PVA-5.4%Ag, b) PVA-3.8%Ag
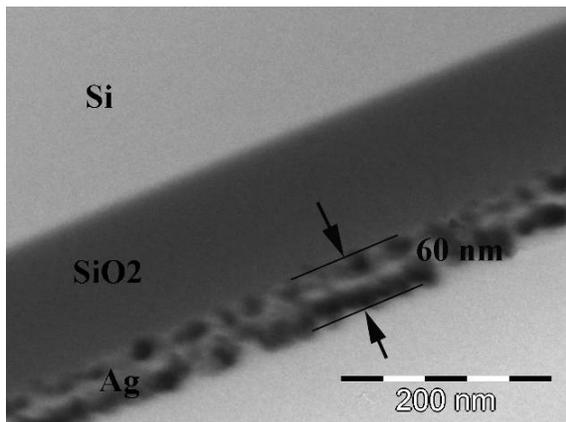
Fig. 9. XTEM image of PVA-Ag film at the interface with silicon wafer substrate.

AFM analysis indicates very low roughness (<1-2 nm) of all layers. This indicates that the layers have very good surface planarity, suitable for photonic waveguides and circuits.

3.3 Patterned structures

Experiments for patterning lenses, optical waveguides, diffractive optical elements and microfluidic channels have been carried out using EBL (for very low doped PMMA based nanocomposites) and microtransfer molding for the other nanocomposites.

Fig. 10 presents a SEM image of lens shape nanostructures obtained by EBL in very low doped (0.5% TiO_2) PMMA double layer (Mw 495K/Mw 950K).

Fig. 11 shows the profile of a 15 µm wide channel obtained in TiO_2 doped PMMA by microtransfer molding. The master was obtained in SU-8 (fig. 12 a) by optical lithography and the mold (fig. 12 b) in PDMS by cast molding. One can see that the replica reproduce the master dimensions.

Other optical components (microprism, optical waveguides and microlenses) obtained in highly doped (10% TiO_2) PMMA by transfer molding or replica molding are presented in fig. 13 and fig. 14.
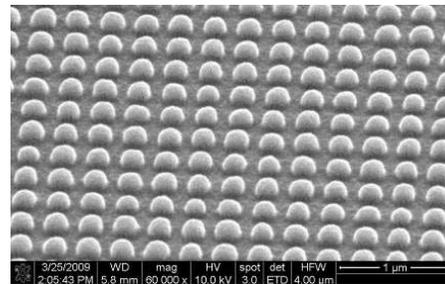
Fig.10. SEM image of a low doped PMMA layer patterned by EBL to obtain lens-shape nanostructures.
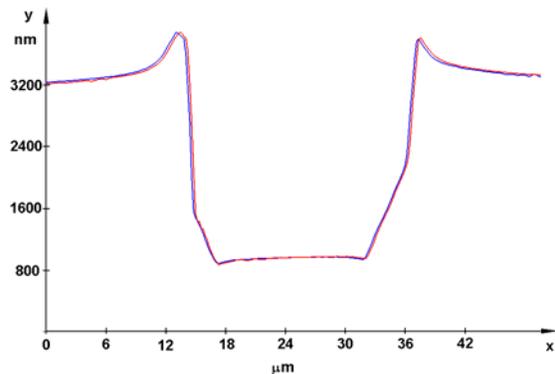
Fig. 11. AFM Profile of a channel obtained in TiO_2 doped PMMA by microtransfer molding.
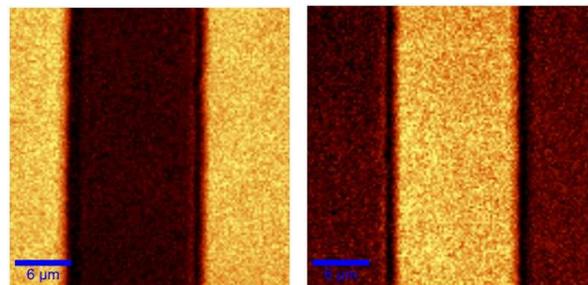
a)   b)

Fig.12. Confocal images of the SU-8 original (a), and of the PDMS mold (b) for microtransfer molding
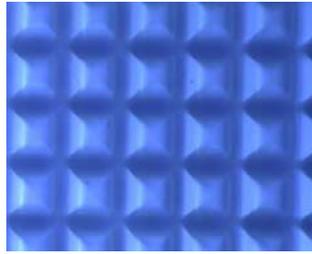
a)
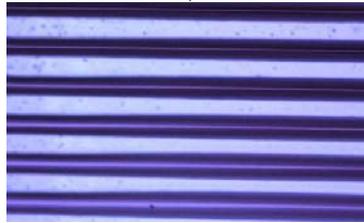
b)

Fig. 13. Optical images of diffractive optical elements (a) and optical waveguides obtained in in PMMA-TiO_2 by transfer molding
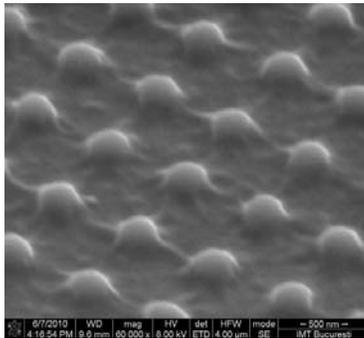
Fig. 14. SEM image of lens-shaped nanostructured obtained in TiO_2 doped PMMA by replica molding.

Microtransfer molding was also used to pattern Rhodamine-doped PMMA. The replica in doped PMMA was transferred on a glass substrate. Fig. 15 shows a fluorescence image of a waveguide in PMMA doped with Rhodamine obtained on a glass substrate by microtransfer molding.
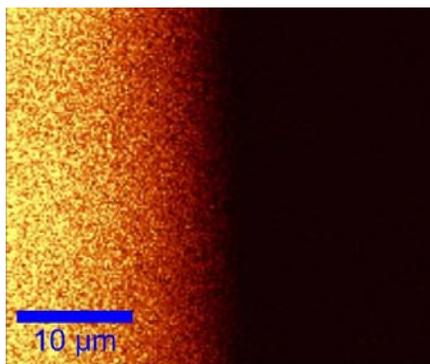
Fig. 15. Fluorescence image of a structure patterned in Rhodamine doped PMMA by microtransfer molding.

An optical image of a PMMA layer doped with photoinitiator and TiO_2, patterned by optical lithography (UV exposure, $7 mW/cm^2$) is given in fig. 16. Unfortunately, the sensitivity of the PMMA film doped with TiO_2 and UV photoinitiator is not good enough. The exposed areas were only partly developed. The process has to be further investigated in order to optimize the dopants concentration and the exposure/development parameters.
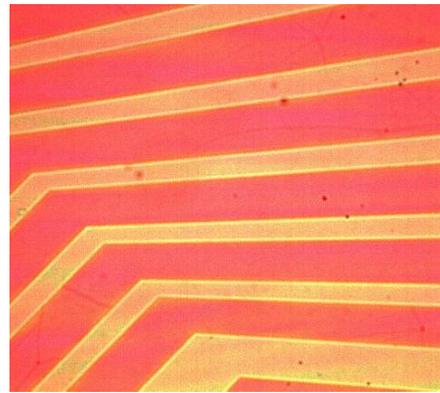
Fig. 16. Optical image of the PMMA-TiO2_UV initiator layer patterned by UV lithography

4. Conclusions

PMMA-TiO_2, PMMA-ZrO_2 nanocomposites were prepared by sol-gel process. The nanocomposites films were characterized by UV-VIS spectroscopy and ellipsometry to determine the transmittance, the refractive index and the thickness of the thin film. The size and the dispersion of the nanoparticles in the polymer matrix were determined using transmission electron microscopy and atomic force microscopy. Layers with high refractive index (1.5 -1.8), good thickness uniformity and optical quality surface were obtained. The dopant nanoparticles have a diameter in the range 5-10 nm and are uniformly distributed in the PMMA polymer matrice. The size of nanoparticles and the refractive index depend on metal oxide contend in nanocomposite.

The very low doped PMMA layers can be patterned using EBL, while for highly doped layers other techniques have to be developed. In this case microtransfer molding based on a resits master and PDMS mold was used.

TiO_2 doped PMMA can be UV-patterned if a photoinitiator is added, but the process require further investigations.

PVA-Ag nanocomposites have been developed using a chemical route, by in-situ formation of metal nanoparticles within the polymer matrix. It has been observed that the nanoparticles tend to aggregate and form clusters during the preparative process; the refractive index of PVA-Ag films depend on Ag contend in the films, while the size of nanoparticles (6-

20 nm) seems to be not depend on the Ag contend. These films shows a low absorbance for λ >600 nm and a high refractive index (>1.75).

All the experimented films, having high refractive index and good transmittance can be used to fabricate photonic components.

Acknowledgments

References

[1] J. K. Lee, Y. M. Wang, S. Cho, F. Wudl, A. J. Heeger, Organic Electronics **10**, 1223 2009

[2] B.O'Regan, M.Grätzel, Nature **353**, 737 (1991)

[3] S. Günes, N. S. Sariciftci, Inorganica Chimica Acta **361**, 581 (2008).

[4] F. W. Mont, J. K. Kim, Martin F. Schubert, E. Fred Schubert, R. W. Siegel, J.Appl.Phys. **103**, 083120 (2008).

[5] X. Fan, I. M. White, S. I. Shopova, H. Zhu, J. D. Suter, Y. Sun, Analytica chimica acta **620**, 8 (2008).

[6] K.Y. Pu, B. Liu, Biosensors and Bioelectronics **24**, 1067 (2009)

[7] L. Criante , R. Castagna, F. Vita , D. E. Lucchetta, F. Simoni, J. Opt. A: Pure Appl. Opt. **11**, 024011 (2009).

[8] S. Rath, M. Heilig, H. Port, J. Wrachtrup, Nano Lett. **7**(12), 3845 (2007).

[9] Y. Hu, Z. Zhang, Y. Chen, Q. Zhang, W.Huang, Optics Letters **35**, 46 (2010).

[10] S.Balslev, A. Mironov, D. Nilsson, A. Kristensen, OPTICS EXPRESS **14**, 2170 (2006).

[11] L. Menon, W. T. Lu, A. L. Friedman, S. P. Bennett, D. Heiman, S. Sridhar, Applied Physics Letters **93**, 123117 (2008).

[12] W.S. Kim, K. B. Yoon, B.S. Bae, J. Mater. Chem. **15**, 4535 (2005).

[13] Walter Caseri, Chemical Engineering Communications, 196, 549;

[14] S. Srivastava, M. Haridas, J. K. Basu, Bull. Mater. Sci. **31**, 213 (2008).

[15] C. Paquet, E. Kumacheva, Materialstoday **11**, 48 (2008).

[16] T. Hanemann, J. Boehm, C. Müller, E. Ritzhaupt-Kleissl, Proc. of SPIE **6992**, 69920D (2008).

[17] Y. Xia, G. M. Whitesides, Annual Rev. Mater. Sci. **28**, 153 (1998).

[18] C. S. Wu, C. F. Lin, H. Y. Lin, C. L. Lee, C. D. Chen, Adv. Mater. **19**, 3052 (2007).

[19] Blümel, A. Klug, S. Eder, U. Scherf, E. Moderegger, E. J. W. List, Organic Electronics **8**, 389 (2007).

[20] G. A. DeRose, L. Zhu, J. K.S. Poon, A. Yariv, A. Scherer, Microelectronic Engineering **85**, 758 (2008).

[21] J. Marques-Hueso, R.Abargues, J.Canet-Ferrer, J. L. Valdes, J. Martinez-Pastor, Microelectronic Engineering **87**, 1147 (2010).

[22] S. A. Maier Plasmonics: Fundamentals and Applications, Springer 2007, chapter.5

_____
*Corresponding author: paula.obreja@imt.ro